Research Article

Photocatalytic Activity of Nanosized Cadmium Sulfides Synthesized by Complex Compound Thermolysis

Yingchun Yu, Youxian Ding, Shengli Zuo, and Jianjun Liu

Faculty of Sciences, Beijing University of Chemical Technology, Beijing 100029, China

Correspondence should be addressed to Jianjun Liu, jjliu717@yahoo.com.cn

The nanosized cadmium sulfides (CdSs) containing different phase structures were synthesized via the complex compound thermolysis method using different molar ratio of thiourea to acetate cadmium (S/Cd) and characterized by XRD, TEM, UV-Vis, and IR spectra. The results of photocatalytic degradation of rhodamine B (RB) show that the activity order of CdS concerning the phase compositions is of cubic > hexagonal > cubic + hexagonal, where the CdS with the cubic phase has the best photocatalytic degradation activity of RB due to its larger abilities of adsorption and absorbance and smaller particle size of about $10 \sim 13$ nm.

1. Introduction

Nanomaterials are assemblies with particles or crystal size between 1 nm and 100 nm, which include different types of nanoparticles, nanowires, nanotubes, and nanofilms and other nanobulk materials. Nanomaterials possess many unique physical and chemical properties different from their bulk counterparts due to the obvious quantum size effect and small size effect [1, 2]. Photocatalysis is one of the key technologies to solve both energy and environmental problems using solar energy, in which an efficient photocatalyst is necessary. Although remarkable progress has been made in recent years for photocatalysts working under ultraviolet light, there are limitations for the photocatalysts to be applied under visible light. The problem could be resolved by using visible light-induced photocatalysts with proper band gap energy, such as CdS, WO_3, or Fe_2O_3. Although CdS is a good candidate for photocatalytic water reduction and pollutant oxidation, it has the fatal photocorrosion problem due to the oxidation of itself by the photogenerated hole [3]. Usually, CdSs are of cubic phase and hexagonal phase and the cubic phase can transform into hexagonal one when heated to certain temperatures [4]. At present, there are many studies on the synthesis of hexagonal CdS. Lin et al. [5] and Bao et al. [6] found that the hexagonal

CdS nanoparticles synthesized via solvothermal method have much better photocatalytic activity for degradation of methylene blue and better hydrogen production activity for water photolysis, using thiourea and cadmium acetate as raw materials. Jing and Guo [7] reported a CdS catalyst system with a high hydrogen production activity for water photolysis using cadmium acetate as cadmium source and H_2S as sulfur source. The CdS synthesized under solvothermal or heating conditions is usually of stable hexagonal phase, but there are a few reports on the synthesis of metastable cubic CdS. Many factors can influence the photocatalytic activity of CdS, such as phase composition, crystallite size, morphology, specific surface area, and energy gap. For example, Degussa P25 (made in Germany), a type of commercial nanosized titania which possesses a high photocatalytic activity, exists in polymorphs composed of about 80% anatase and 20% rutile [8]. Therefore, it is very important to study how to get the CdS photocatalysts with different phase compositions and their photocatalytic activities by controlling reaction conditions.

In this study, the CdS nanocrystals with different phase compositions were synthesized via thermal decomposition of thiourea-cadmium complexes using cadmium acetate and thiourea as raw materials. The photocatalytic activities of the synthesized CdS nanocrystals for the degradation of Rhodamine B under visible light were also studied.
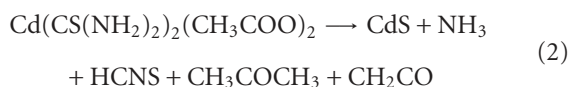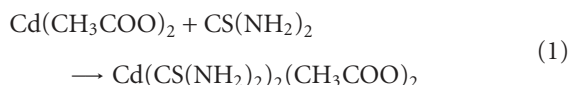
TABLE 1: Synthesis conditions, phase composition, and crystalline size of CdS photocatalysts.

Sample no.	$c(CS(NH_2)_2)/(mol \cdot l^{-1})$	$c(Cd^{2+})/(mol \cdot l^{-1})$	$n(S)/n(Cd)$	Phase composition	Grain size/nm
A	0.07	0.14	0.5	CdS(cubic) + CdO	10
B	0.14	0.14	1	Cubic	13
C	0.21	0.14	1.5	Cubic + hexagonal	17
D	0.28	0.14	2	Hexagonal	26
E	0.42	0.14	3	Hexagonal	26

*The grain size of CdS can be calculated by using the crystal plane of cubic (111) and hexagonal (002), respectively.

2. Experimental

2.1. Synthesis of CdS.

All chemicals were of analytical grade and used without further purification. The preparation conditions and analysis results of CdS samples synthesized using different S/Cd ratios are listed in Table 1. The synthesis procedure of nanosized CdS was as follows: (a) to prepare a series of aqueous solutions including $CS(NH_2)_2$ and $Cd(CH_3COO)_2$ according to their concentration listed in Table 1; (b) 50 mL $CS(NH_2)_2$ solution was dropped into 50 mL $Cd(CH_3COO)_2$ solution to form transparent solution under stirring for 30 min and then heated at 100°C for 10 h so as to get a yellow single resource complex precursor of $Cd(CS(NH_2)_2)_2(CH_3COO)_2$ (1) which will turn to CdS after calcination at 300°C for 0.5 h. All other products were gaseous (2). Thus there are no any other byproducts in the thermolysis process. The final products were washed twice by ethanol and deionized water followed by drying at 100°C for 10 h. The synthesized CdS samples are used after grinding to powder,

$$Cd(CH_3COO)_2 + CS(NH_2)_2$$
$$\longrightarrow Cd(CS(NH_2)_2)_2(CH_3COO)_2 \tag{1}$$

$$Cd(CS(NH_2)_2)_2(CH_3COO)_2 \longrightarrow CdS + NH_3$$
$$+ HCNS + CH_3COCH_3 + CH_2CO \tag{2}$$

2.2. Characterization of Photocatalysts.

The powder X-ray diffraction (XRD) patterns were recorded on a Rigaku D/MAX-2500 diffractometer with Cu K_α ($\lambda = 1.5406$ Å) radiation. The transmission electron microscope (TEM) images were taken on a Hitachi800 electron microscope. The UV-vis diffuse reflectance spectra were measured on a Shimadzu UV-2550 spectrometer. The FT-IR spectra of the samples dispersed in KBr pellets were obtained within the 4000–400 cm^{-1} wavenumbers on a Nicolet 370MCT spectrometer.

2.3. Photocatalytic Testing.

A 500-W Xe lamp was used as the light source and the visible wavelength was controlled through a 420-nm cut filter (LF420, China), which was hanged in a dark box and kept at about 15 cm above the liquid level. Aqueous suspensions of Rhodamine B (RB) dye (100 mL, with an initial concentration of 1.5×10^{-4} M) and photocatalyst powder (100 mg) were placed in a 250 mL beaker. Prior to irradiation, the suspensions were magnetically stirred for 10 min under dark condition to
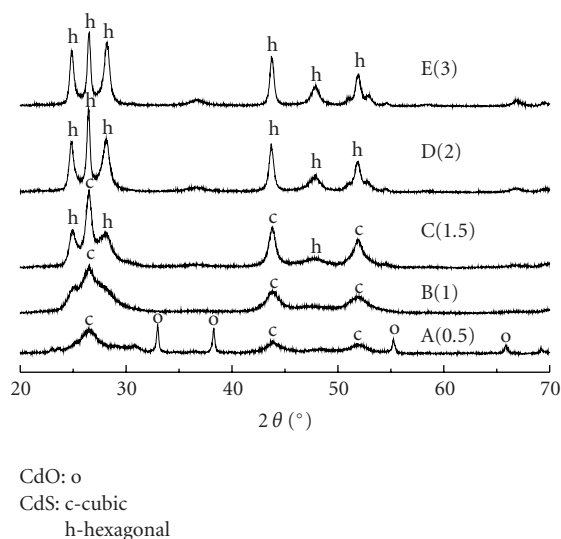

CdO: o
CdS: c-cubic
    h-hexagonal

FIGURE 1: XRD patterns of CdS samples synthesized by different $n(S)/n(Cd)$ ratios of A : 0.5, B : 1, C : 1.5, D : 2, and E : 3.

establish an adsorption/desorption equilibrium between dye and photocatalyst surface. Under stirring, aliquots of a small amount of suspension (about 4 mL) were taken out every 10 minutes under irradiation conditions, then centrifuged and analyzed using a SP-2000UV spectrophotometer (made in China).

3. Results and Discussion

3.1. XRD Characterization.

XRD patterns of the CdS products are depicted in Figure 1. All the diffraction peaks of the nanocrystals are well indexed either as cubic CdS (JCPDF # 65-2887) or as hexagonal CdS (JCPDF # 77-2306) which have been marked by the symbol "c" or "h." When increasing thiourea/Cd molar ratio from 0.5 to 1, 1.5, 2, and then to 3, a mixture of cubic CdS and CdO (Figure 1A), a cubic CdS (Figure 1B), a mixture of cubic and hexagonal CdS (Figure 1C), and hexagonal CdS (Figures 1D and 1E) were obtained, respectively.

The crystal phase of synthesized CdS changes regularly, from cubic phase → mixed phase → hexagonal phase. With the thiourea/Cd molar ratio of 0.5, the excess cadmium acetate decomposes into CdO under heating condition. During the process of reaction, the cadmium acetate and thiourea molecules form a single source precursor of
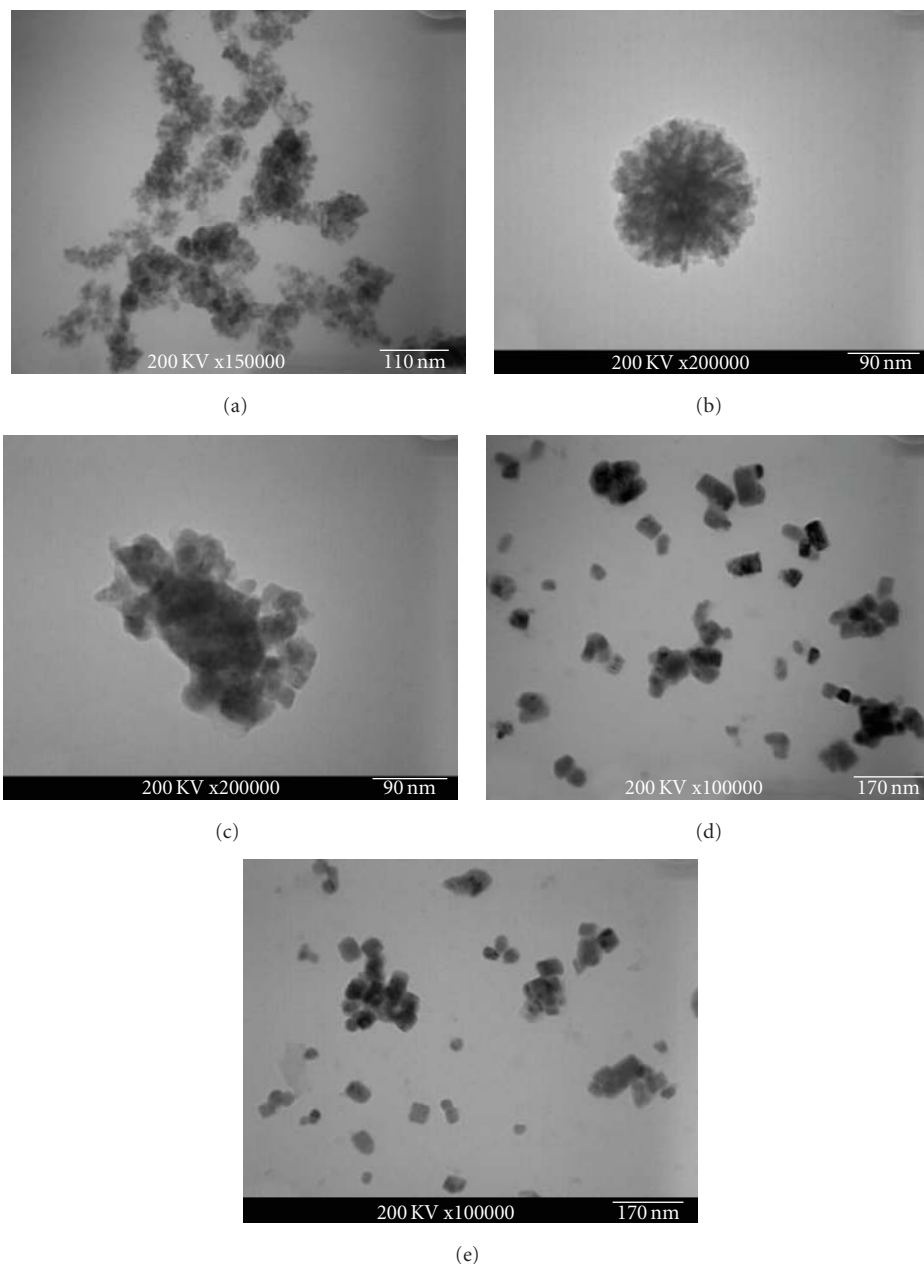
(a)

(b)

(c)

(d)

(e)

FIGURE 2: TEM images of CdS samples synthesized by different $n(S)/n(Cd)$ ratios of A : 0.5, B : 1, C : 1.5, D : 2, and E : 3.

Cd-thiourea complex $Cd(SC(NH_2)_2)_2(CH_3COO)_2$, in which the Cd ion coordinates with four S atoms to form tetrahedral CdS_4 block. In the cubic zinc blende structure, the pairs of interpenetrating tetrahedra are in the staggered conformation, while in the hexagonal wurtzite structure, these tetrahedra are in the eclipsed conformation. In the present study, for the Cd-thiourea-CH_3COO—complex with a low thiourea/Cd ratio, the symmetry of the ligands is low, and there are steric hindrances to the formation of the S_3Cd-SCd_3 group in the eclipsed conformation [9]. Thus, the lower symmetry of the first coordination sphere of Cd in a thiourea complex leads to a lower symmetry of the cubic CdS structure. In contrast, there are no such hindrances for the

Cd-thiourea-CH_3COO—complex with a large thiourea/Cd ratio, and CdS crystallizes in the hexagonal wurtzite structure [10], which is thermodynamically more stable.

With increased S/Cd molar ratio, the grain size of CdS increases from 10 nm of the cubic phase (Figure 1A), to 26 nm of the hexagonal phase (Figure 1E), as shown in Table 1, that indicates that the change of grain size is an important factor affecting the phase transition of CdS [11] except for the symmetry change abovementioned.

3.2. TEM Characterization. The TEM images of CdS samples synthesized with different S/Cd ratios were shown in Figure 2. It is shown that the particles of sample A consisting
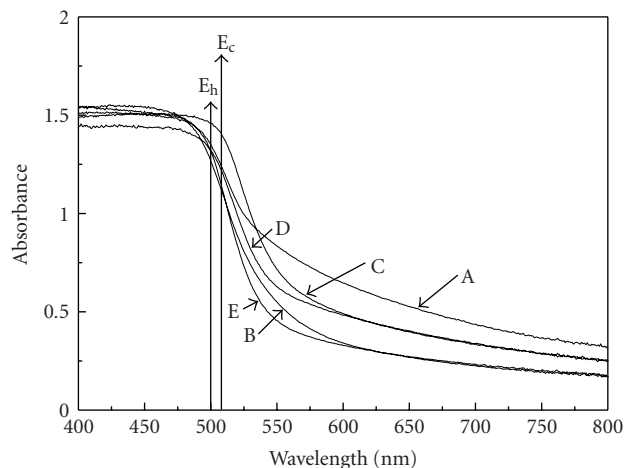
FIGURE 3: UV-vis spectra of CdS samples synthesized by different $n(S)/n(Cd)$ ratios of A : 0.5, B : 1, C : 1.5, D : 2, and E : 3.

FIGURE 4: IR spectra of CdS samples synthesized by different $n(S)/n(Cd)$ ratios of A : 0.5, B : 1, C : 1.5, D : 2, and E : 3.

of CdO and cubic CdS are about 10 nm exhibiting chain-like aggregates. The morphology of sample B seems as flocculent flower with diameter of about 100 nm which is consisting of much smaller particles and fiber aggregates. In the center of sample C, a number of particles with the diameter of 10 to 20 nm are separated out corresponding to the mixed phases of cubic and hexagonal CdS, as shown in Figure 1C. With increased S/Cd molar ratio, the morphology of the samples becomes more perfect and homogeneous crystal of cubic CdS with diameter of about 20~30 nm that is a good agreement in the calculation results (Table 1), as shown in Figures 2(d) and 2(e). It is worth mentioning that the morphologies of CdS change subtly with a gradual increase of S/Cd ratio, suggesting that the S/Cd ratio plays a key role in the formation of diverse CdS nanostructures.

3.3. UV-Vis Characterization.

All CdS samples synthesized with different S/Cd ratios show strong light absorption at the wavelength of less than 550 nm, and the consequent weak absorption even extends to 800 nm, as shown in Figure 3 which indicates that the CdS samples have broad light absorption in the whole visible region. The absorbance has the order of: A > (C, D) > (B, E), in which samples A and C are the mixed phase of cubic CdS and CdO, or of cubic and hexagonal CdS, respectively, while sample B is the pure cubic CdS, and samples D and E are pure hexagonal CdS. It is well known that the intrinsic energy gap of pure cubic or hexagonal CdS is $E_{cubic} = 2.41$ eV or $E_{hexagonal} = 2.47$ eV [12], corresponding to the cutoff absorption wavelength of E_c ($\lambda = 515$ nm) or E_h ($\lambda = 502$ nm), respectively, as shown by the vertical lines in Figure 3. Thus all CdS samples synthesized with different S/Cd ratios undergo a redshift compared to the intrinsic adsorption of cubic or hexagonal CdS.

3.4. IR Characterization.

The absorption bands of 3300–3400 cm^{-1} and 1607–1645 cm^{-1} are assigned to the N–H stretching and -NH$_2$ bending vibrations of thiourea molecule [13], respectively, whose intensities gradually
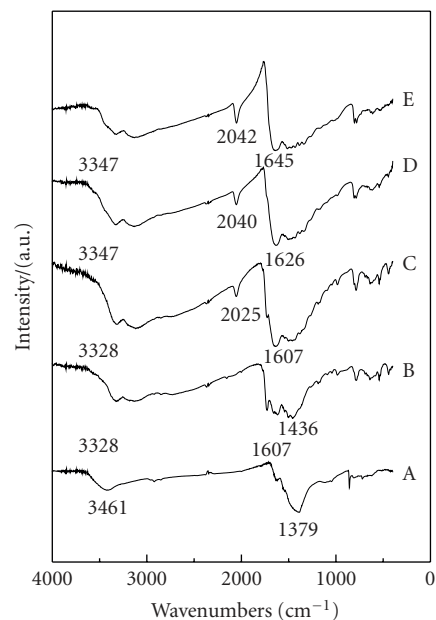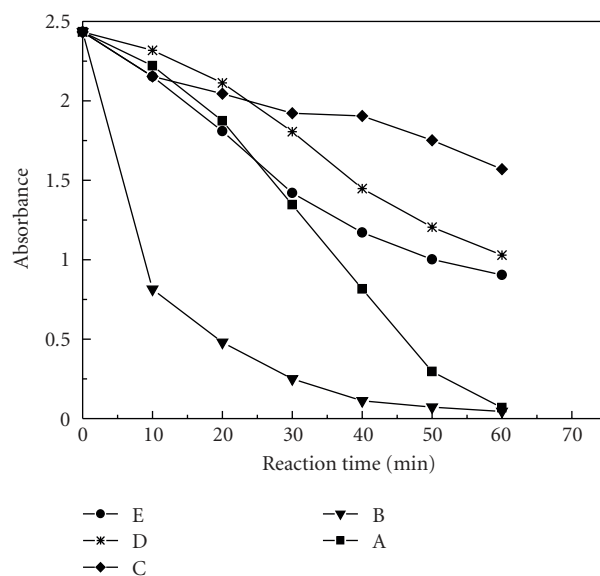

FIGURE 5: Photocatalytic degradation curves of RB using CdS samples synthesized by different $n(S)/n(Cd)$ ratios of A : 0.5, B : 1, C : 1.5, D : 2, and E : 3.

increase with increasing S/Cd ratios, as shown in Figure 4. Similarly, the absorption bands of 2040 cm^{-1} also gradually increase in samples of C, D, and E, which is attributed to the infrared vibration of –C≡N bond of thiocyanate (HCNS, H–S–C≡N) produced in reaction (2). However, the characteristic diffraction peaks of thiocyanate or its derivatives do not appear in Figure 1, which indicates that the real content of decomposed products in the CdS sample is very low (<1%). In contrast to the above situation, the IR absorption peaks near 2040 cm^{-1} of thiocyanate do not

appear in the samples of A(0.5) and B(1.0), indicating that there is no excess thiourea to be decomposed into thiocyanate.

3.5. Photocatalytic Activities. The curves of photocatalytic degradation of RB using different CdS samples are shown in Figure 5. With the residual absorbance of RB after 60 min as evaluation index, the degradation activity is in the order of $B \approx A > E > D > C$. Sample B has relatively rapid degradation within the first 10 min, which can be attributed to its strong adsorption of RB due to the flocculent particle morphology with larger surface area, as shown in Figure 2(b). Furthermore, sample A has the strongest absorption in visible region and the smallest grain size (10 nm), so it has a higher photocatalytic activity. While $n(S)/n(Cd) > 1$, the catalytic activities of samples E, D, and C are lower than that of A and B. It is known from Figure 4 that the excess thiocyanate remains on the surface of samples E, D, and C, in which the S^{2-} ions can act as a photoinduced hole sacrificial reagent and compete with the oxidation of RB dye, resulting in the decrease of the photocatalytic activity [14]. On the other hand, the order of phase composition effect on the catalytic activity is cubic > hexagonal > mixed. As shown in Figure 2, the hexagonal CdS samples of D and E are in good crystallinity and homogeneous particle dispersion. However, the mixed phase CdS of C is an aggregate containing many defects between the two-phase interface, accounting for the lower photocatalytic activity.

4. Conclusions

The cubic CdS, hexagonal CdS, and their mixed phase were synthesized under the conditions of thiourea/Cd (S/Cd) molar ratios (0.5~3) of ≤ 1, ≥ 2, and 1.0~1.5, respectively. The grain size of CdS increases with the increased S/Cd ratio. The photocatalytic activity is in order of cubic > hexagonal > mixed phase, in which the cubic phase CdS has the best photocatalytic activity for RB degradation due to its strong adsorption, intense absorbance in visible region, and the smaller grain size.
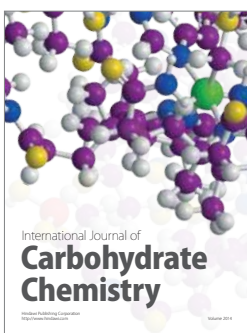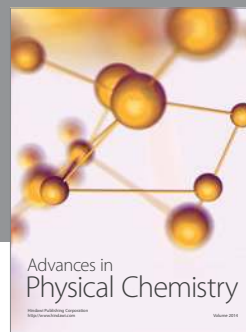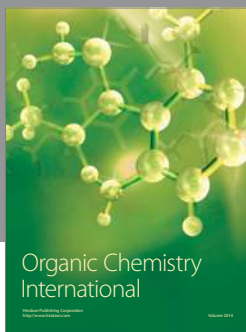
Acknowledgments

References

[1] W. Kelsall, I. W. Hamley, and M. Geoghegan, *Nanoscale Science and Technology*, John Wiley & Sons, New York, NY, USA, 2005.

[2] C. P. Poole and F. J. Owens, *Introduction to Nanotechnology*, John Wiley & Sons, New York, NY, USA, 2003.

[3] D. Meissner, R. Memming, and B. Kastening, "Photoelectro-chemistry of cadmium sulfide. 1. reanalysis of photocorrosion and flat-band potential," *Journal of Physical Chemistry*, vol. 92, no. 12, pp. 3476–3483, 1988.

[4] N. Sahu, M. K. Arora, S. N. Upadhyay, and A. S. K. Sinha, "Phase transformation and activity of cadmium sulfide photocatalysts for hydrogen production from water: role of adsorbed ammonia on cadmium sulfate precursor," *Industrial and Engineering Chemistry Research*, vol. 37, no. 12, pp. 4682–4688, 1998.

[5] G. Lin, J. Zheng, and R. Xu, "Template-free synthesis of uniform CdS hollow nanospheres and their photocatalytic activities," *Journal of Physical Chemistry C*, vol. 112, no. 19, pp. 7363–7370, 2008.

[6] N. Bao, L. Shen, T. Takata et al., "Facile Cd—thiourea complex thermolysis synthesis of phase-controlled CdS nanocrystals for photocatalytic hydrogen production under visible light," *Journal of Physical Chemistry C*, vol. 111, no. 47, pp. 17527–17534, 2007.

[7] D. Jing and L. Guo, "A novel method for the preparation of a highly stable and active CdS photocatalyst with a special surface nanostructure," *Journal of Physical Chemistry B*, vol. 110, no. 23, pp. 11139–11145, 2006.

[8] J. Liu, W. Qin, S. Zuo, Y. Yu, and Z. Hao, "Solvothermal-induced phase transition and visible photocatalytic activity of nitrogen-doped titania," *Journal of Hazardous Materials*, vol. 163, no. 1, pp. 273–278, 2009.

[9] A. V. Naumov, V. N. Semenov, and E. G. Goncharov, "Properties of CdS films prepared from thiourea complexes of cadmium salts," *Inorganic Materials*, vol. 37, no. 6, pp. 539–543, 2001.

[10] V. Swayambunathan, D. Hayes, K. H. Schmidt, Y. X. Liao, and D. Meisel, "Thiol surface complexation on growing CdS clusters," *Journal of the American Chemical Society*, vol. 112, no. 10, pp. 3831–3837, 1990.

[11] N. Herron, Y. Wang, and H. Eckert, "Synthesis and characterization of surface-capped, size-quantized CdS clusters. Chemical control of cluster size," *Journal of the American Chemical Society*, vol. 112, no. 4, pp. 1322–1326, 1990.

[12] D. J. Kim, Y.-M. Yu, J. W. Lee, and Y. D. Choi, "Investigation of energy band gap and optical properties of cubic CdS epilayers," *Applied Surface Science*, vol. 254, no. 22, pp. 7522–7526, 2008.

[13] G. W. C. Kaye and T. H. Laby, *Tables of Physical and Chemical Constants*, Longman Press, London, UK, 16th edition, 1995.

[14] I. Tsuji, H. Kato, and A. Kudo, "Photocatalytic hydrogen evolution on ZnS-CuInS$_2$-AgInS$_2$ solid solution photocatalysts with wide visible light absorption bands," *Chemistry of Materials*, vol. 18, no. 7, pp. 1969–1975, 2006.

International Journal of
Medicinal Chemistry

Organic Chemistry
International

International Journal of
Photoenergy

International Journal of
Analytical Chemistry

Advances in
Physical Chemistry

International Journal of
Carbohydrate Chemistry

Journal of
Quantum Chemistry

The Scientific World Journal

Hindawi

Submit your manuscripts at
http://www.hindawi.com

Journal of
Analytical Methods
in Chemistry

Journal of
Spectroscopy

International Journal of
Inorganic Chemistry

International Journal of
Electrochemistry

Journal of
Applied Chemistry

Bioinorganic Chemistry
and Applications

Journal of
Theoretical Chemistry

Chromatography
Research International

Journal of
Catalysts

Journal of
Chemistry

International Journal of
Spectroscopy